Electronic Supplementary Information

Rapid and stable complexation of the α-generators bismuth-212 and lead-212 with a tetraazamacrocyclic chelator bearing thiosemicarbazone pendant arms

Melyssa L. Grieve,[a,b] Patrick R. W. J. Davey,[c] Paul V. Bernhardt,[d] Craig M. Forsyth[a] and Brett M. Paterson*[b,d]

[a]School of Chemistry, Monash University, Clayton, VIC 3800, Australia.
[b]Centre for Advanced Imaging, Australian Institute for Bioengineering and Nanotechnology, The University of Queensland, Brisbane, QLD 4072, Australia
[c]Department of Chemistry, Simon Fraser University, Burnaby, BCV5A 1S6, Canada.
[d]School of Chemistry and Molecular Biosciences, The University of Queensland, Brisbane, QLD 4072, Australia.

*Corresponding author: brett.paterson@uq.edu.au

Table of Contents

Structure Characterisation

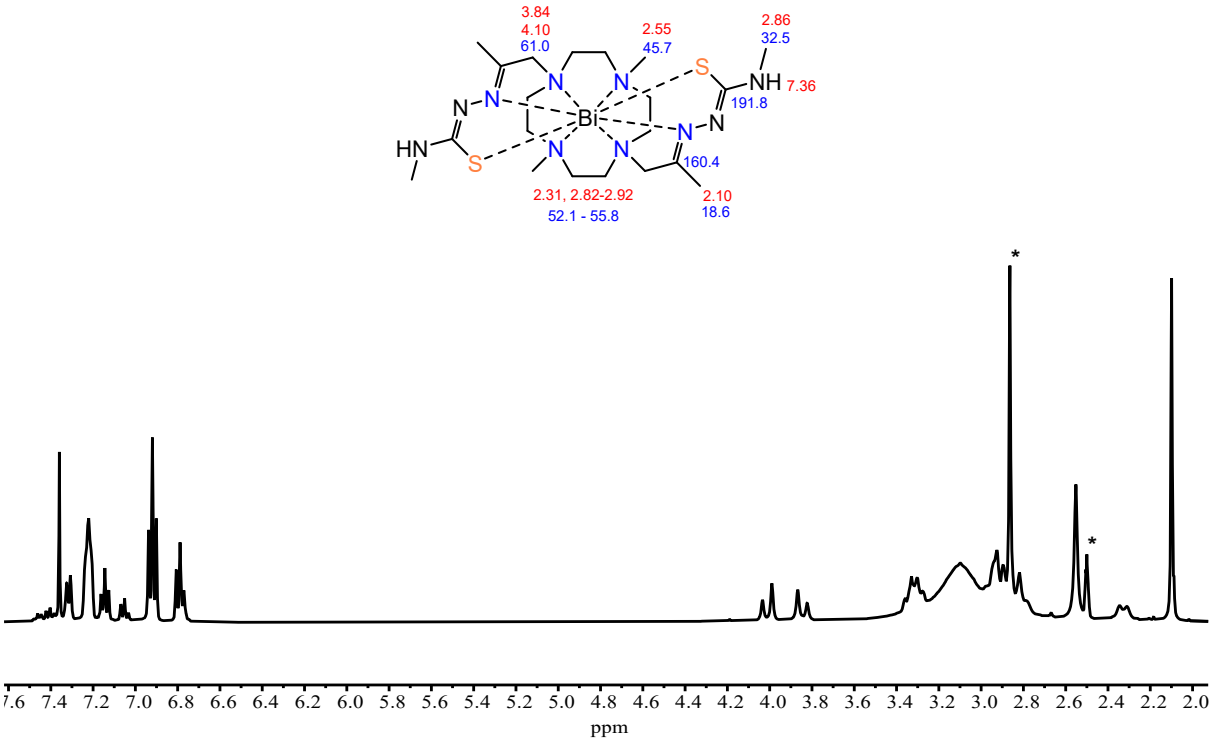

Figure S1 The ^{1}H NMR spectra of [Bi(DOTS)](BPh$_4$) in d_6-DMSO at 373 K.

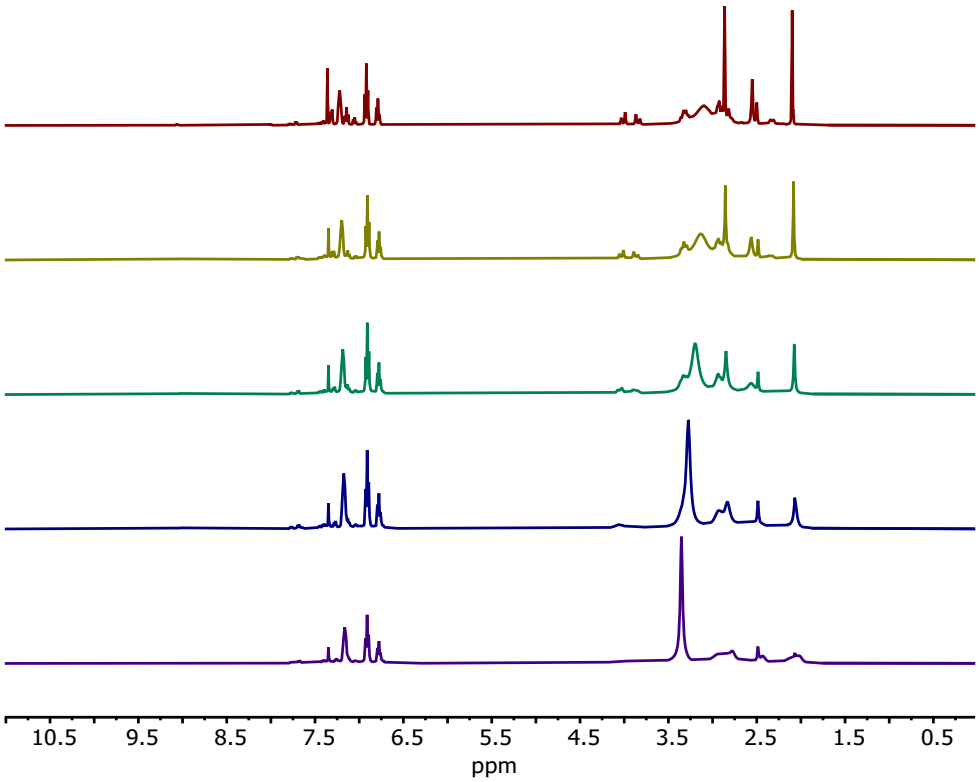

Figure S2 The ^{1}H NMR spectra of [Bi(DOTS)](BPh$_4$) in d_6-DMSO at 298 K (bottom), 318 K, 338 K, 358 K and 373 K (top).

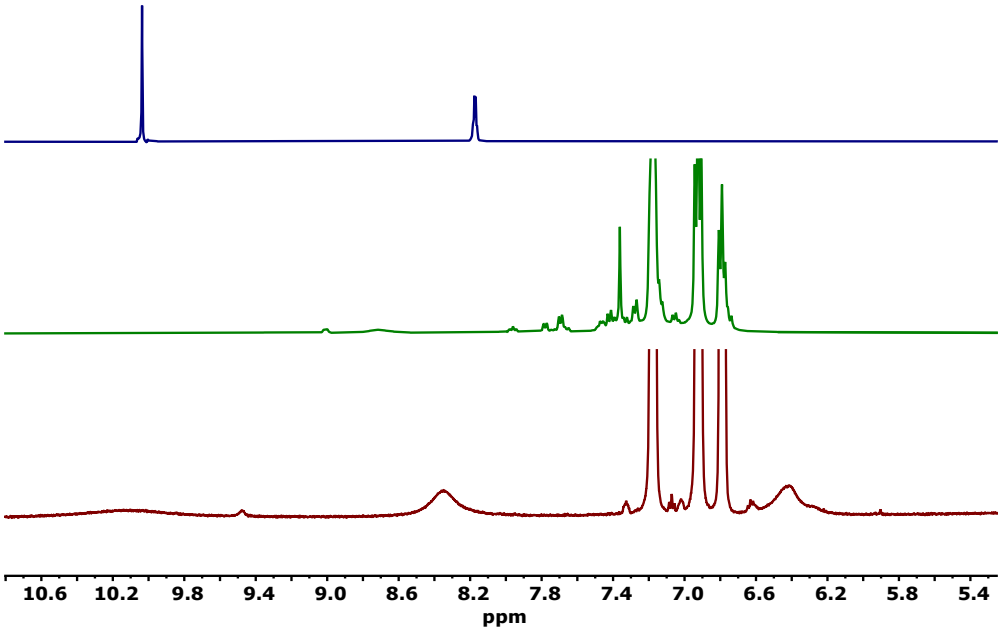

Figure S3 The ^{1}H NMR spectra from 5 - 10.7 ppm of H_2DOTS (top), [Bi(DOTS)](BPh_4) (middle) and [Pb(H_2DOTS)]$(OAc)_x(BPh_4)_y$ (bottom) in d_6-DMSO at 298 K.

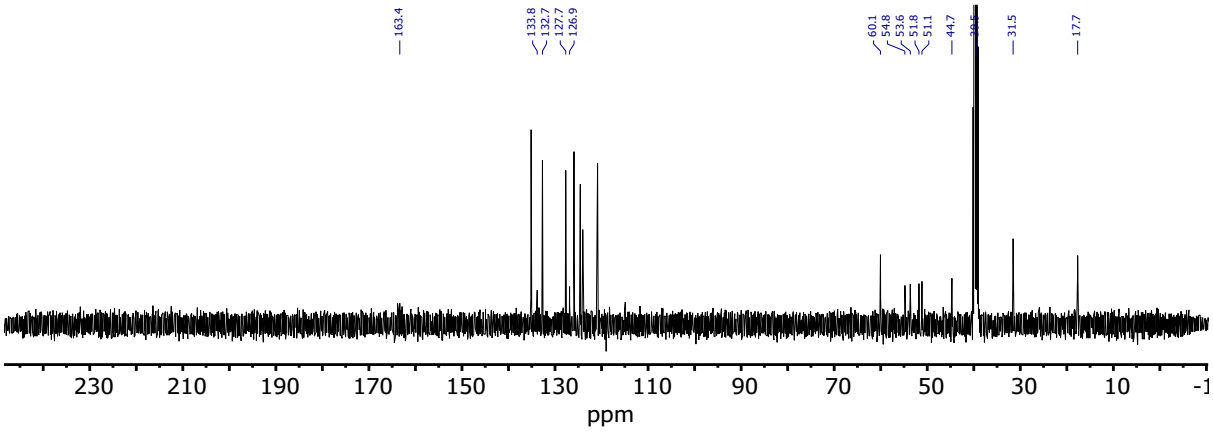

Figure S4 The ^{13}C{^{1}H} NMR spectra of [Bi(DOTS)](BPh_4) in d_6-DMSO at 373 K.

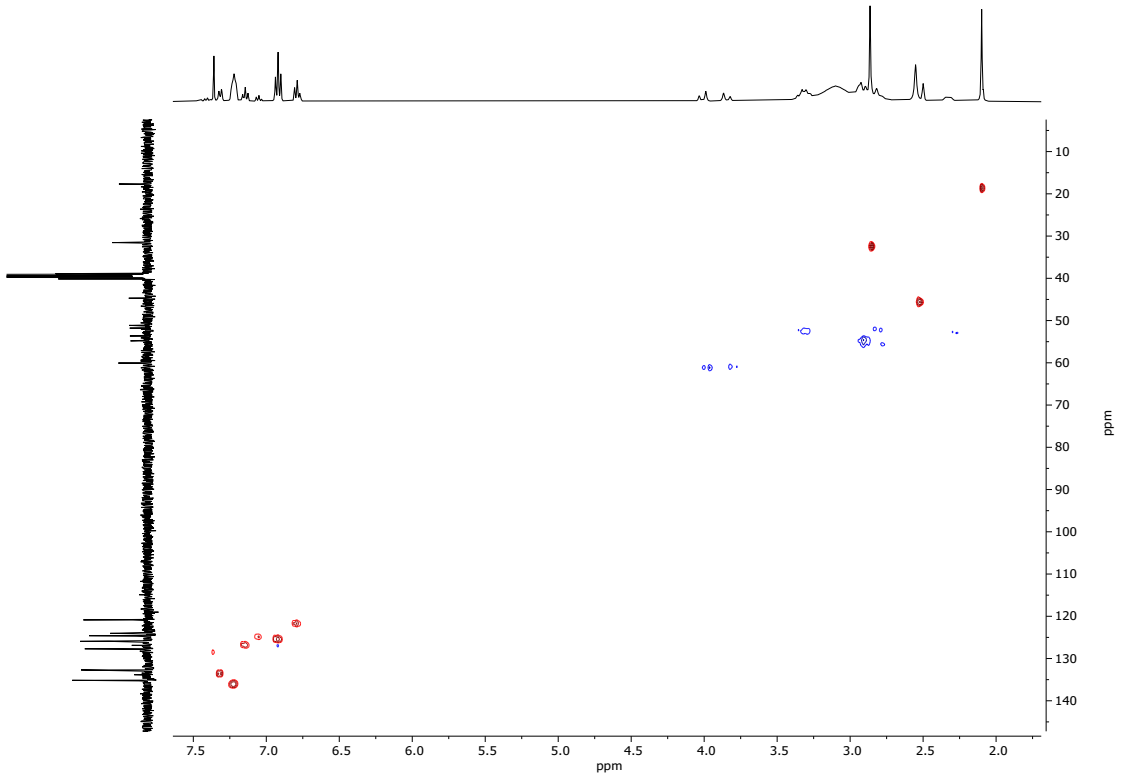

Figure S5 The ^{13}C-^{1}H HSQC spectra of [Bi(DOTS)](BPh$_4$) in d_6-DMSO at 373 K. The red color shows the proton-carbon correlations in –CH– and –CH$_3$ groups while the blue color shows the proton-carbon correlations in –CH$_2$– groups.

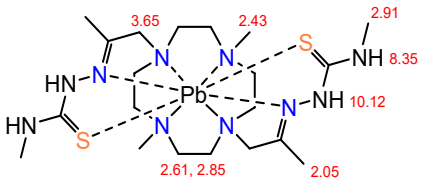

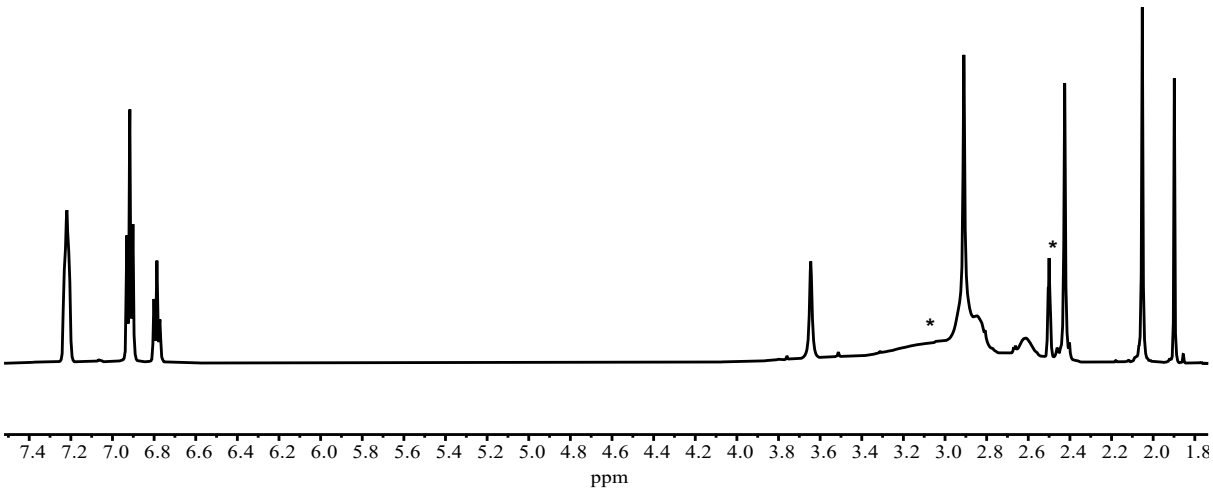

Figure S6 The ^{1}H NMR spectra of [Pb(H$_2$DOTS)](OAc)$_x$(BPh$_4$)$_y$ in d_6-DMSO at 373 K.

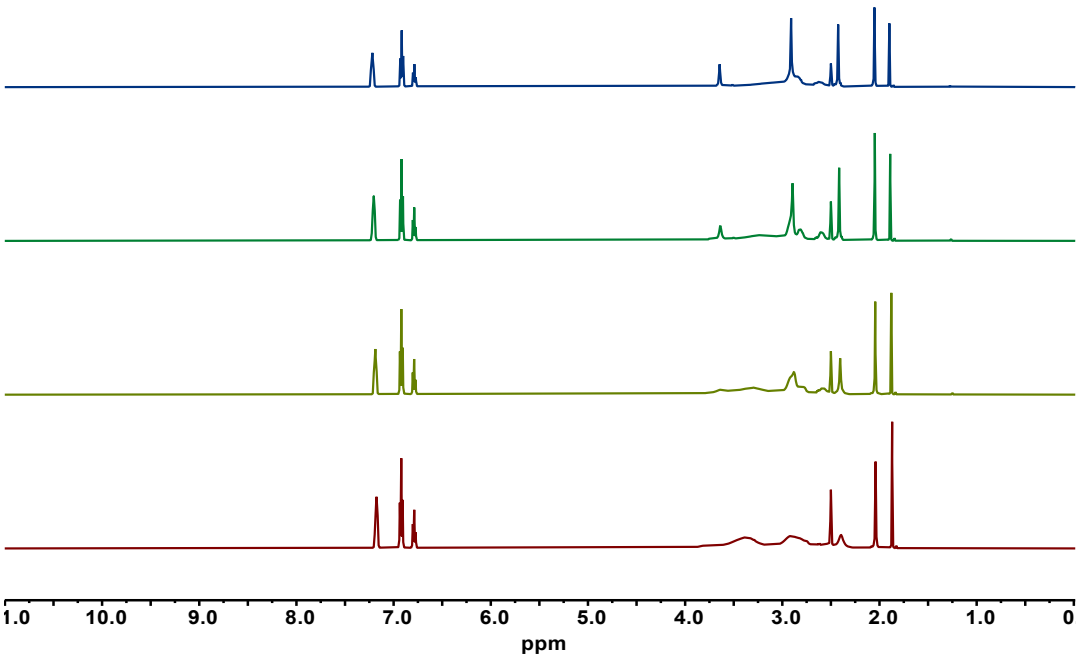

Figure S7 The ^{1}H NMR spectra of $[Pb(H_2DOTS)](OAc)_x(BPh_4)_y$ in d_6-DMSO at 298 K (bottom), 323 K, 348 K and 373 K (top).

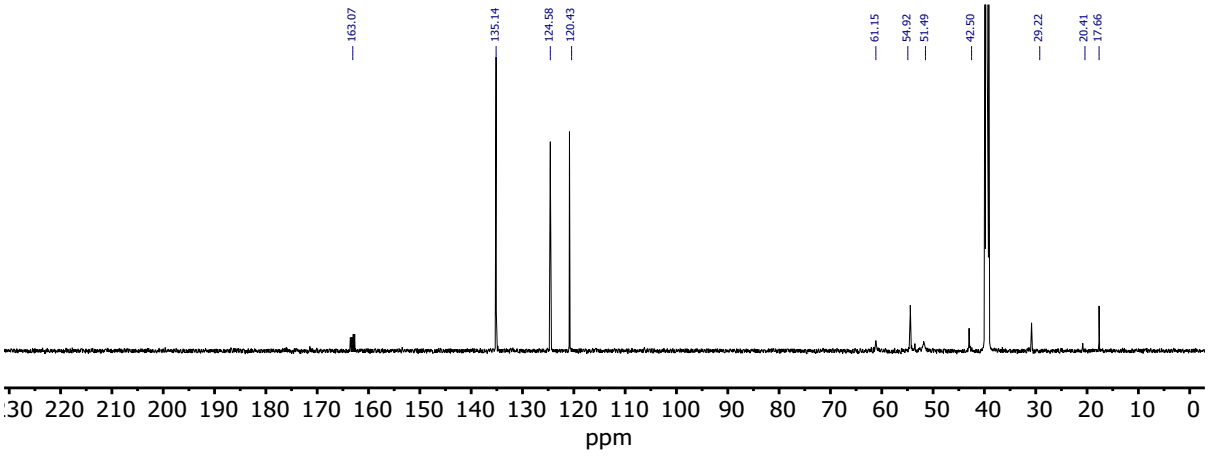

Figure S8 The $^{13}C\{^{1}H\}$ NMR spectra of $[Pb(H_2DOTS)](OAc)_x(BPh_4)_y$ in d_6-DMSO at 373 K.

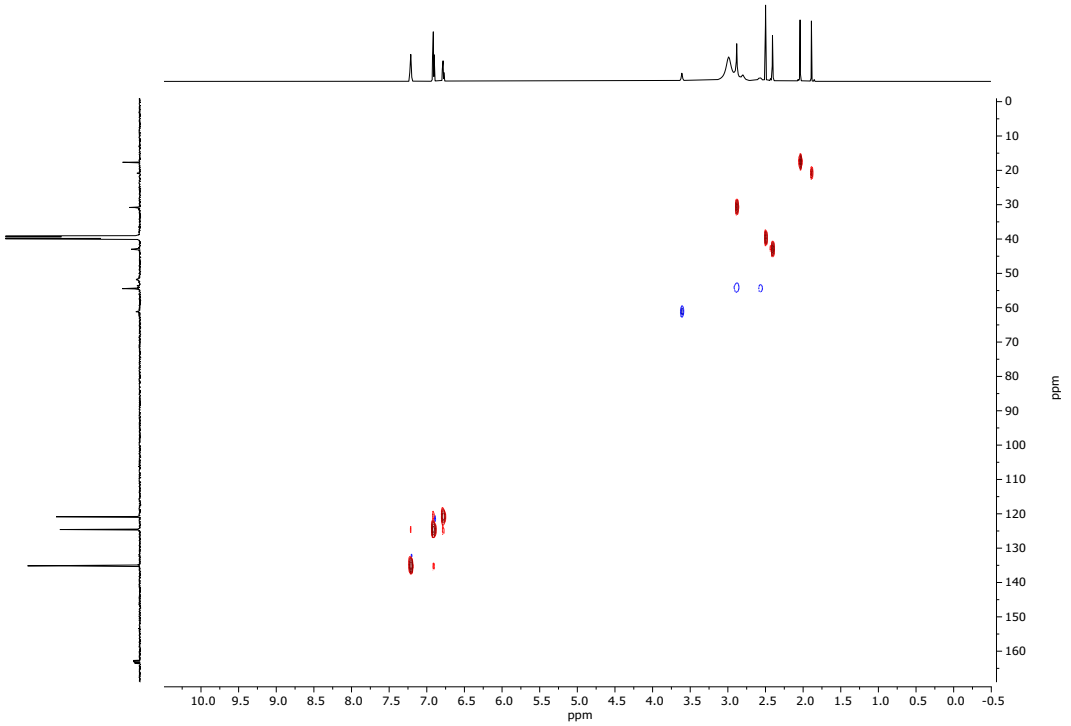

Figure S9 The ^{13}C-^{1}H HSQC spectra of $[Pb(H_2DOTS)](OAc)_x(BPh_4)_y$ in d_6-DMSO at 373 K. The red color shows the proton-carbon correlations in –CH– and $–CH_3$ groups while the blue color shows the proton-carbon correlations in $–CH_2–$ groups.

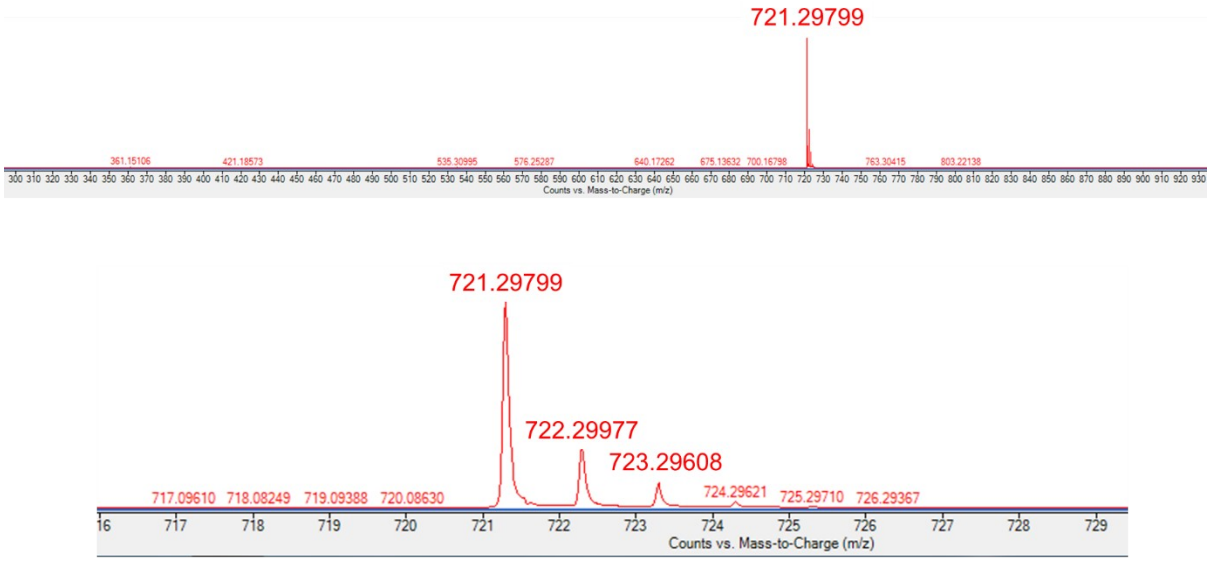

Figure S10 The high-resolution mass spectrum (ESI^+) of $[Bi(DOTS)]^+$

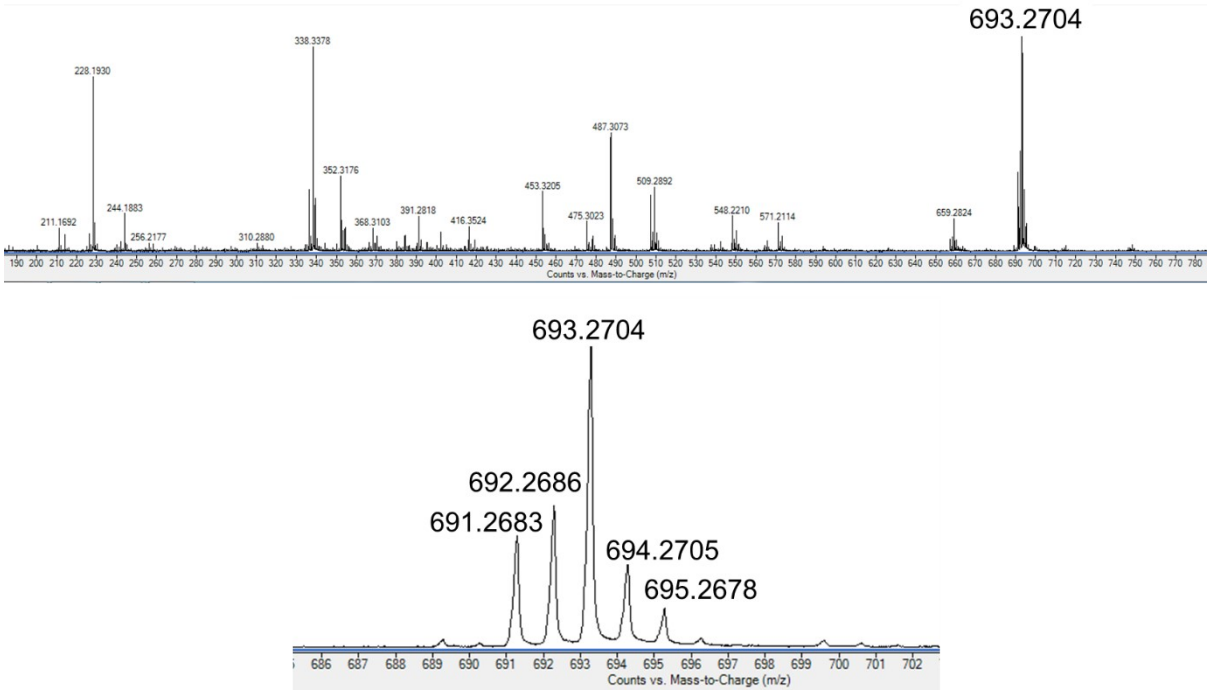

Figure S11 The high-resolution mass spectrum (ESI$^+$) of $[Pb(H_2DOTS) - H^+]^+$

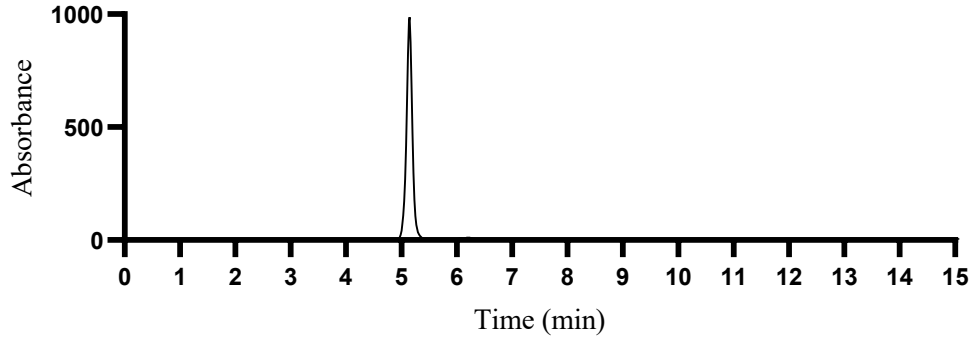

Figure S12 RP-HPLC (λ = 280 nm) of $[Bi(DOTS)]^+$

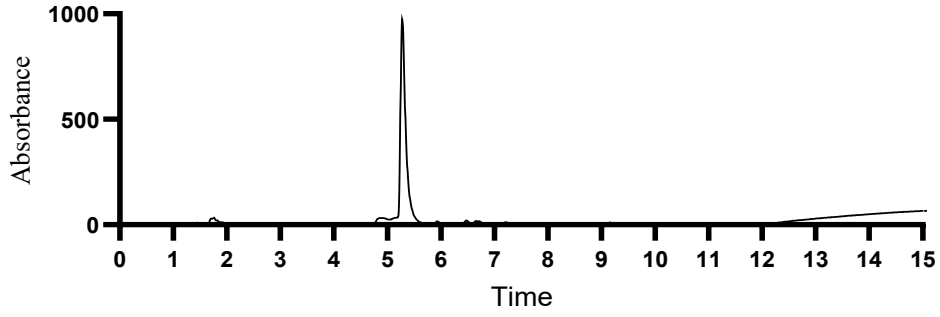

Figure S13 RP-HPLC (λ = 254 nm) of $[Pb(H_2DOTS)]^{2+}$

Table S1 Crystallographic and refinement data for [Bi(DOTS)](BPh_4) and [Pb(H_2DOTS)](BPh_4)$_2$·2DMSO

Parameter	**[Bi(DOTS)](BPh_4)**	**[Pb(H_2DOTS)](BPh_4)$_2$·2DMSO**
Formula	$C_{44}H_{60}BBiN_{10}S_2$	$C_{72}H_{90}B_2PbO_5N_{10}S_4$
Formula Weight (Å^3)	1014.94	1532.58
Crystal System	Tetragonal	Monoclinic
Space Group	*I*4/*m*	*P*2/*n*
Temperature (K)	123 K	190 K
a (Å)	12.4557(1)	9.9835(5)
b (Å)	12.4557(1)	13.6709(8)
c (Å)	36.8615(8)	28.353(1)
α (°)	90	90
β (°)	90	93.292(4)
γ (°)	90	90
V (Å^3)	5718.86	3863.3(3)
Z	4	2
ρ (g cm^{-3})	1.179	1.317
Absorption coefficient (μmm^{-1})	6.995	5.671
F(000)	2064	1576
Angle range (°)	3.7050 - 76.6680	4.4690 – 55.3700
Reflections collected	15531	21216
Independent reflections	3060 [0.0434]	6004 [0.1364]
Final R1 values (I > 2σ(I))	0.0355	0.0782
Final wR1(F2) values (I > 2σ(I))	0.0903	0.1725
Final R1 values (all data)	0.0378	0.1131
GOOF	1.084	1.028

Speciation

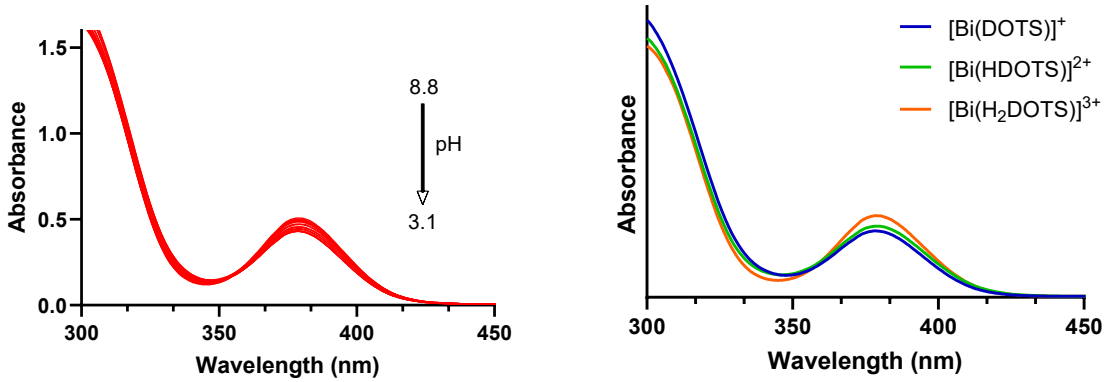

Figure S14 UV-Visible spectra of $[Bi(DOTS)]^{+}$ over the pH range 3.1 – 8.8 (left). The calculated UV-Visible spectra of each species identified during the pH titration (right). Data analysed using ReactLab EQUILIBRIA.

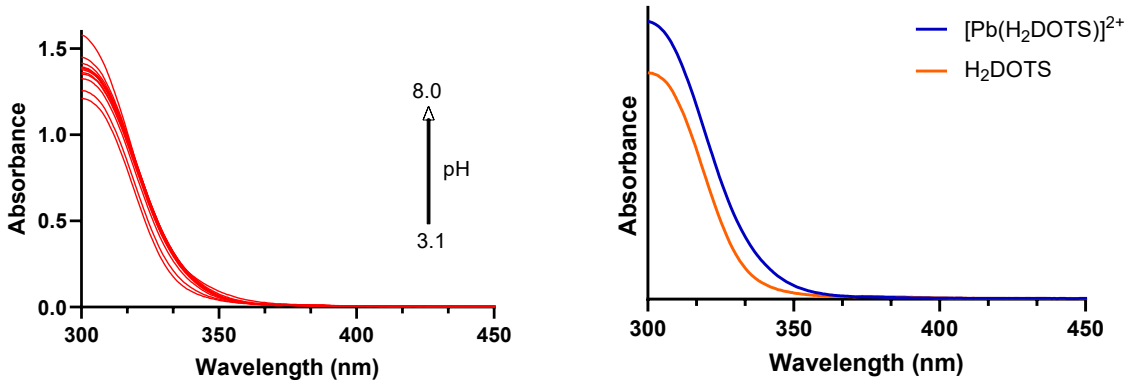

Figure S15 UV-Visible spectra of $[Pb(H_2DOTS)]^{2+}$ over the pH range 3.1 – 8.0 (left). The calculated UV-Visible spectra of each species identified during the pH titration (right). Data analysed using ReactLab EQUILIBRIA.

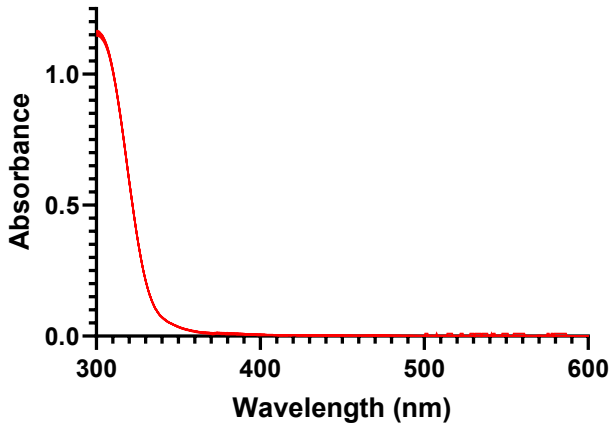

Figure S16 UV-Visible spectra of H_2DOTS collected over the pH range 3-9.

Dissociation Kinetics

The kinetic inertness of $[Bi(DOTS)]^+$ was tested using a competition against 100 equivalents of H_5DTPA at 25 °C in 30% DMSO in acetate buffer (pH 5) (**Figure S17**). $[Bi(DOTS)]^+$ demonstrated exceptional kinetic inertness to the H_5DTPA challenge experiment remaining 100% intact after 4 days and 85% intact after 45 days.

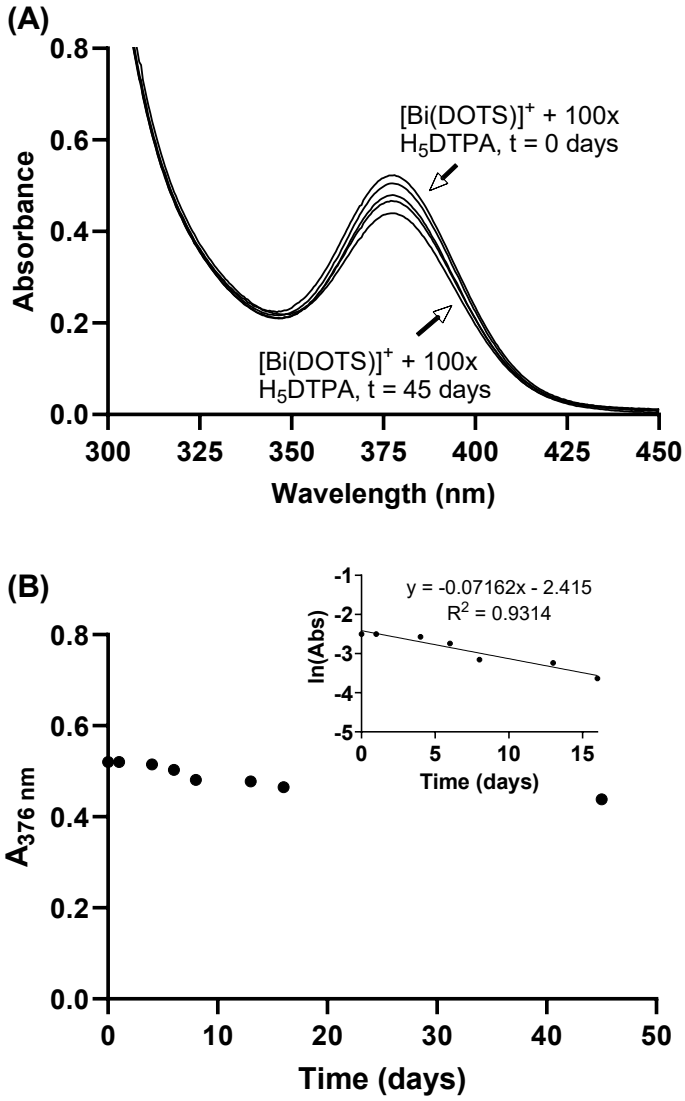

Figure S17 (A) Time course of the UV-visible absorbance spectra of $[Bi(DOTS)]^+$ in the presence of 100 equivalents of H_5DTPA in 30% DMSO/ 0.5 M acetate buffer (pH 5) after 0, 6, 8, 16 and 45 days (approximately 84% of the $[Bi(DOTS)]^+$ complex remained intact after 45 days). (B) Plot of the change in absorbance at 376 nm vs. time. Inset: Fit of the data to a first order process.

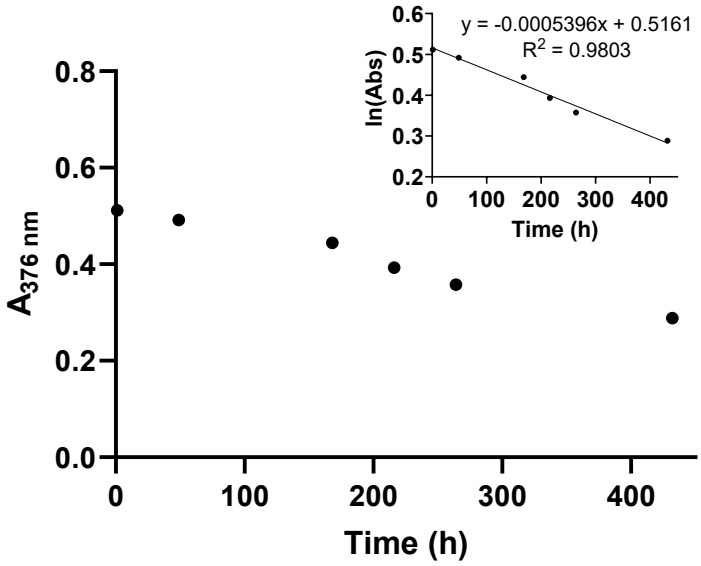

Figure S18 Plot of the change in absorbance at 376 nm vs. time of the UV-visible absorbance spectra of $[Bi(DOTS)]^+$ in the presence of 1000 equivalents of H_5DTPA in 20% DMSO/0.02 M MOPS buffer (pH 7.4) (approximately 61% of the $[Bi(DOTS)]^+$ complex remained intact after 18 days). Inset: Fit of the data to a first order process.

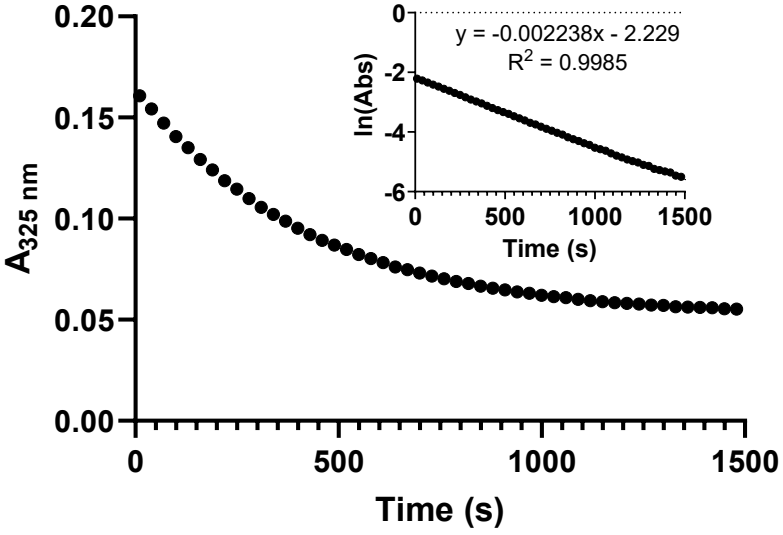

Figure S19 Plot of the change in absorbance at 325 nm vs. time of the UV-visible absorbance spectra of a solution of $[Pb(H_2DOTS)]^{2+}$ in the presence of 1000 equivalents of H_5DTPA in 30% DMSO/0.02 M MOPS buffer (pH 7.4) at 25 °C. Spectra obtained at 30 sec intervals. Inset: Fit of the data to a first order process.

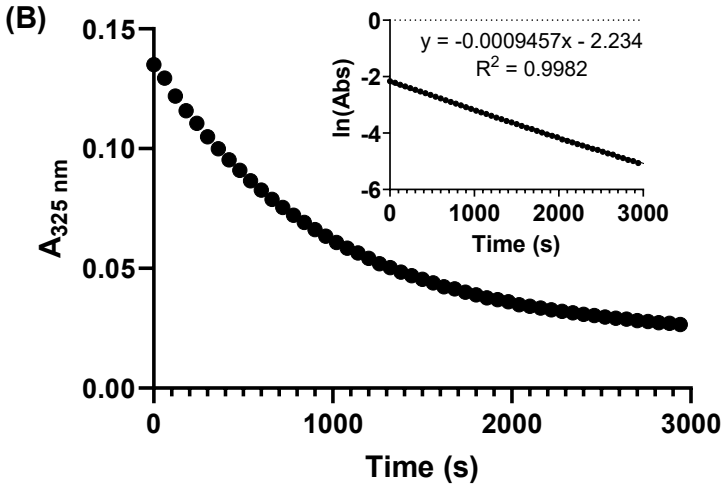

Figure S20 Plot of the change in absorbance at 325 nm vs. time of the UV-visible absorbance spectra of a solution of $[Pb(H_2DOTS)]^{2+}$ in the presence of 100 equivalents of H_4EDTA in 1% DMSO/pH 7.4 MOPS buffer at 25 °C. Spectra obtained at 1 min intervals. Inset: Fit of the data to a first order process.

Density Functional Theory Calculations

Assessing the thermodynamics of $[Pb(H_2DOTS)]^{2+}$ and $[Bi(DOTS)]^{+}$

The relative stabilities of the radiometal complexes, i.e. the Gibbs free energies of the reaction (ΔG) between the H_2DOTS chelator to Bi^{3+} and Pb^{2+}, were assessed by density functional theory (DFT) calculations according to the designed equation (1). Under these conditions, *n* is the charge of the cation, *m* is the charge of the competing ion, and *x* is the charge of the ligand in the complexation reactions. For Pb^{2+} and Bi^{3+}, the hydration number used was 8 based on previously established experimental and theoretical findings of the likely coordination numbers of Pb^{2+} and Bi^{3+} in water.

Complex Formation Reactions

$$[M_1(H_2O)_8]^{n+} + L_1^{x-} \rightleftharpoons [M_1L_1]^{n-x} + 8H_2O$$

$$\Delta G_1 = G([M_1L_1]^{n-x}) + 8G(H_2O) - G([M_1(H_2O)_8]^{n+}) - G(L_1^{x-}) \quad \textbf{(1)}$$

Table S2 Calculated ΔG (kcal/mol) for complex formation reactions at the BP86-D3/def2-TZVP/IEFPCM(H_2O) level of theory.

Complex	D*G* (kcal/mol)
$[Pb(H_2DOTS)]^{2+}$	-176.51
$[Bi(DOTS)]^{+}$	-360.75

Table S3 Natural Bond Orbital Analysis of the Pb $6s^2$ lone pair in $[Pb(H_2DOTS)]^{2+}$

Complex	Occupancy	Coefficients/Hybrids	Natural Electron Configuration
$[Pb(H_2DOTS)]^{2+}$	1.88466	s(98.96%) p 0.01 (1.03%) d 0.00 (0.01%) f 0.00 (0.00%)	[core]6s(1.90)6p(0.88)6d(0.01)7p(0.04)

Radiolabelling

Table S4 The characteristic γ-rays produced on decay of ^{212}Pb, ^{212}Bi and ^{208}Tl.[66-67] Values <1% probability omitted.

Radionuclide	Energy (keV)	Probability (%)
^{212}Pb	238.63	43.6
	300.09	3.2
^{212}Bi	39.86	1.1
	727.33	6.7
	785.37	1.1
	1620.74	1.5
^{208}Tl	277.37	6.6
	510.74	22.5
	583.19	85.0
	763.45	1.8
	860.53	12.4
	2614.51	99.8

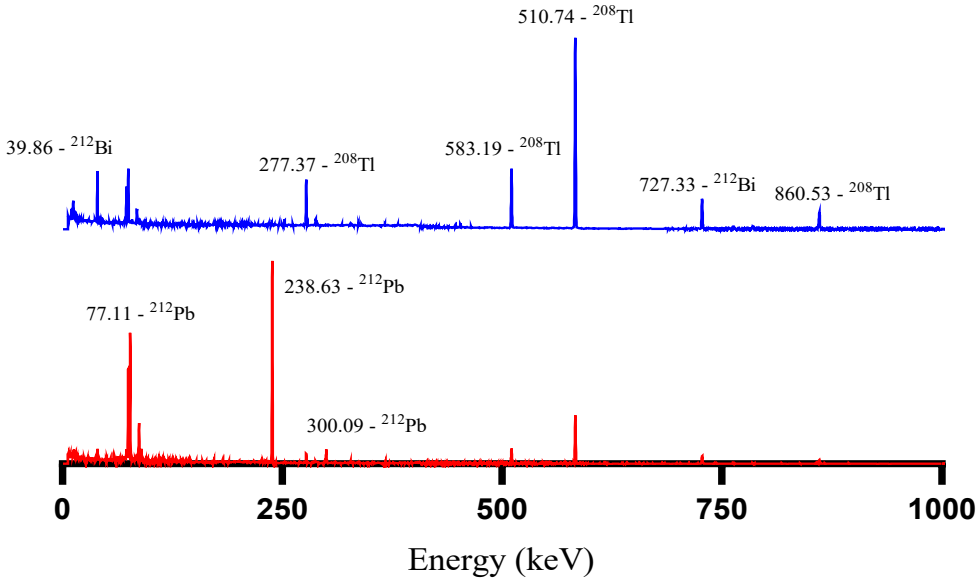

Figure S21 The gamma spectrum of ^{212}Pb in transient equilibrium with daughter radionuclides (red) and separated ^{212}Bi (blue). Significant peaks are labelled with energy (keV) and radionuclide to which they are assigned.

Table S5 The RCC values for $^{212}Pb^{2+}$ with H_2DOTS, H_4TCMC, H_4DOTA and H_4DOTP at different ligand concentrations (10^{-3} - 10^{-7} M) and pH 7.4 (0.1 M HEPES pH 7.4) over 30 min at ambient temperature.

Concentration	H_2DOTS	H_4TCMC[a]	H_4TCMC[b]	H_4DOTA[a]	H_4DOTA[b]	H_4DOTP
10^{-3}	93.7 ± 0.4	95.6 ± 1.4		97.9 ± 1.7		95.6 ± 3.1
10^{-4}	98.9 ± 0.6	98.01 ± 0.04	97.8 ± 0.4	98.7 ± 0.4	97.6 ± 0.1	92.9 ± 6.2
10^{-5}	97.4 ± 1.6	94.6 ± 3.6	98.1 ± 0.5	89.1 ± 7.4	96.5 ± 0.8	85.9 ± 2.9
10^{-6}	77.0 ± 3.9	74.5 ± 6.1	80.8 ± 8.9	7.9 ± 0.7	4.3 ± 1.2	19.1 ± 4.9
10^{-7}	5.0 ± 1.9	3.7 ± 2.5	13.9 ± 1.6	5.6 ± 0.8	3.6 ± 0.5	12.7 ± 13.5

[a]This work. [b]B. L. McNeil, A. K. H. Robertson, W. Fu, H. Yang, C. Hoehr, C. F. Ramogida and P. Schaffer, *EJNMMI Radiopharm. Chem.*, 2021, **6**, 6.

Table S6 The RCC achieved by incubation of $^{212}Pb^{2+}$ with H_2DOTS and H_4DOTP under different ligand concentrations (10^{-3} - 10^{-7} M) at pH 5.5 (0.8 M NH_4OAc pH 5.5) over 30 min at ambient temperature.

Concentration	H_2DOTS	H_4DOTP
10^{-3}	95.9 ± 1.2	94.6 ± 3.1
10^{-4}	96.2 ± 0.8	95.0 ± 3.6
10^{-5}	92.2 ± 0.8	92.5 ± 6.9
10^{-6}	68.9 ± 6.8	26.4 ± 1.5
10^{-7}	3.8 ± 3.0	27.7 ± 4.2

Table S7 The RCC achieved by incubation of $^{212}Bi^{3+}$ 1:1 0.1 M HCl: 0.1 M NaI with H_2DOTS and H_2DOTP under different ligand concentrations at pH 5.5 (0.8 M NH_4OAc pH 5.5) over 10 min at ambient temperature.

Concentration	H_2DOTS[a]	H_4DOTP[a]	H_4DOTP[b]	H_4DOTA[b]
10^{-3}	97.5 ± 2.5	91.8 ± 2.3		
10^{-4}	96.3 ± 2.0	96.6 ± 1.5	92.9 ± 5.6	61.0 ± 7.3
10^{-5}	95.0 ± 3.8	94.4 ± 2.2	87.2 ± 11.8	15.6 ± 6.7
10^{-6}	20.0 ± 1.6	14.5 ± 12.0	89.3 ± 7.2	5.1 ± 4.6
10^{-7}	15.5 ± 4.4	4.4 ± 3.0	85.0 ± 5.2	

[a]This work. [b]J. Simecek, P. Hermann, C. Seidl, F. Bruchertseifer, A. Morgenstern, H. J. Wester and J. Notni, Efficient formation of inert Bi-213 chelates by tetraphosphorus acid analogues of DOTA: towards improved alpha-therapeutics, *EJNMMI Res.*, 2018, **8**, 78. The difference in measured RCC values may be due to a difference in specific activity, but this was not calculated in either case.

Table S8 The RCC achieved by incubation of $^{212}Pb^{2+}$ with H_2DOTS at a ligand concentration of 10^{-4} M at pH 5.5 (0.8 M NH_4OAc pH 5.5) and pH 7.4 (0.1 M HEPES pH 7.4) over 0 - 30 min at ambient temperature.

Time	pH 5.5	pH 7.4
0	0.0 ± 0.0	0.0 ± 0.0
10	97.6 ± 0.8	100.0 ± 0.0
20	96.7 ± 0.4	100 ± 0.0
30	96.6 ± 0.5	100 ± 0.0

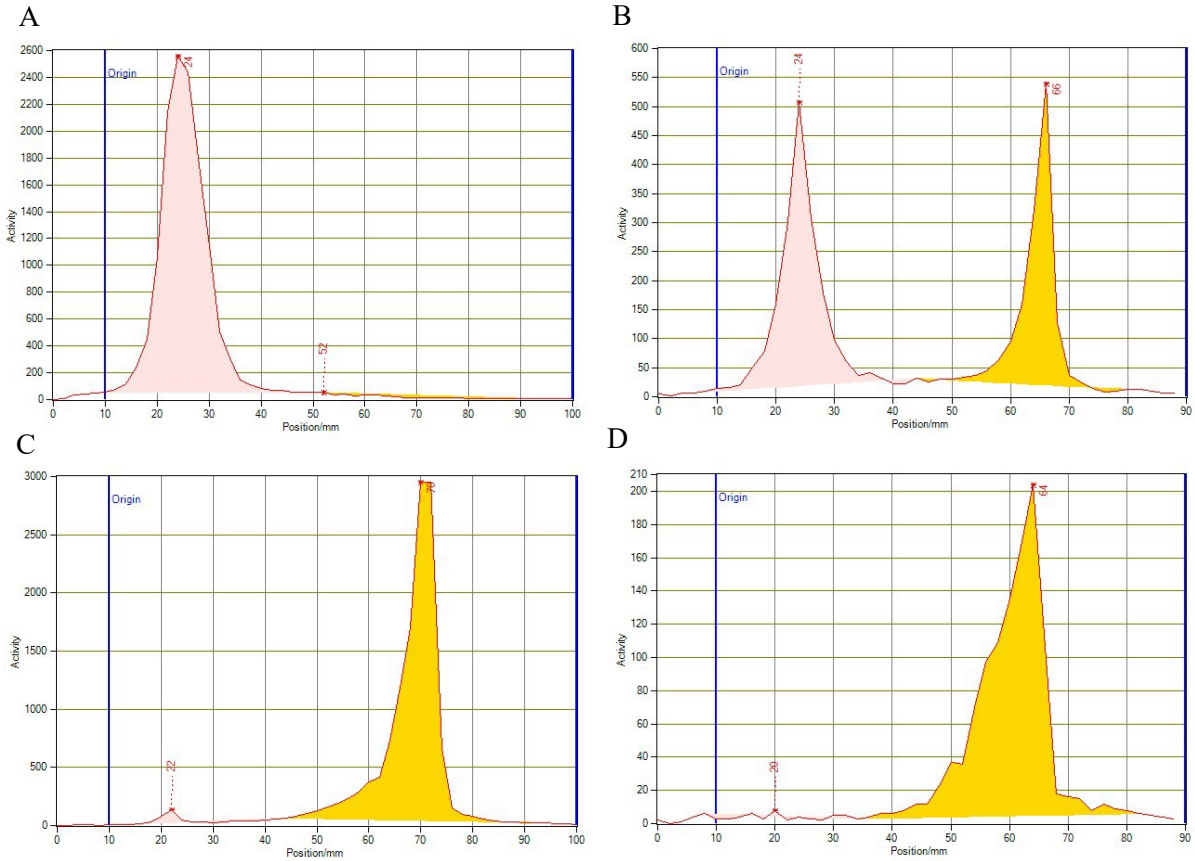

Figure S22. Representative iTLC chromatograms with a 50 mM EDTA mobile phase: A) $[^{212}Pb][Pb(H_2DOTS)]^{2+}$; B) $[^{212}Pb][Pb(H_2DOTS)]^{2+}$ and $[^{212}Pb]Pb^{2+}$; C) $[^{212}Pb]Pb^{2+}$ and; D) $[^{212}Pb]Pb^{2+}$ after incubation in serum for 24 h.

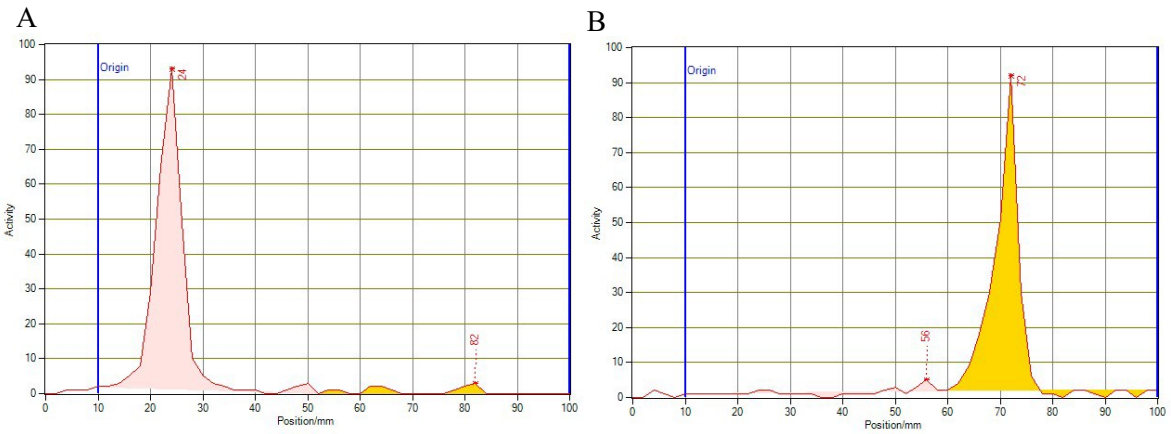

Figure S23. Representative iTLC chromatograms with a 50 mM EDTA mobile phase: A) $[^{212}Bi][Bi(DOTS)]^{+}$ and; B) $[^{212}Bi]Bi^{3+}$.